Effect of obstructions on growing Turing patterns

Cite as: Chaos 32, 073127 (2022); https://doi.org/10.1063/5.0099753 Submitted: 18 May 2022 • Accepted: 27 June 2022 • Published Online: 28 July 2022

Milos Dolnik, Christopher Konow, Noah H. Somberg, et al.

COLLECTIONS

Paper published as part of the special topic on From Chemical Oscillations to Applications of Nonlinear Dynamics: Dedicated to Richard J. Field on the Occasion of his 80th Birthday







ARTICLES YOU MAY BE INTERESTED IN

Dynamical states and bifurcations in coupled thermoacoustic oscillators Chaos: An Interdisciplinary Journal of Nonlinear Science 32, 073129 (2022); https:// doi.org/10.1063/5.0085273

Coexistence of oscillatory and reduced states on a spherical field controlled by electrical potential

Chaos: An Interdisciplinary Journal of Nonlinear Science 32, 073103 (2022); https:// doi.org/10.1063/5.0097010

The Abraham-Lorentz force and the time evolution of a chaotic system: The case of charged classical and quantum Duffing oscillators

Chaos: An Interdisciplinary Journal of Nonlinear Science 32, 073130 (2022); https:// doi.org/10.1063/5.0090477





Effect of obstructions on growing Turing patterns

Cite as: Chaos **32**, 073127 (2022); doi: 10.1063/5.0099753

Submitted: 18 May 2022 · Accepted: 27 June 2022 ·

Published Online: 28 July 2022







Milos Dolnik, De Christopher Konow, Noah H. Somberg, and Irving R. Epstein De De Christopher Konow, Noah H. Somberg, and Irving R. Epstein De De Christopher Konow, Noah H. Somberg, De Christopher Konow, Noah H. So

AFFILIATIONS

Department of Chemistry, MS 015, Brandeis University, Waltham, Massachusetts 02453, USA

Note: This article is part of the Focus Issue, From Chemical Oscillations to Applications of Nonlinear Dynamics: Dedicated to Richard J. Field on the Occasion of his 80th Birthday.

- ^{a)}Also at: Department of Chemistry, Massachusetts Institute of Technology, Cambridge, MA 02139, USA.
- b) Author to whom correspondence should be addressed: epstein@brandeis.edu

ABSTRACT

We study how Turing pattern formation on a growing domain is affected by discrete domain discontinuities. We use the Lengyel-Epstein reaction-diffusion model to numerically simulate Turing pattern formation on radially expanding circular domains containing a variety of obstruction geometries, including obstructions spanning the length of the domain, such as walls and slits, and local obstructions, such as small blocks. The pattern formation is significantly affected by the obstructions, leading to novel pattern morphologies. We show that obstructions can induce growth mode switching and disrupt local pattern formation and that these effects depend on the shape and placement of the objects as well as the domain growth rate. This work provides a customizable framework to perform numerical simulations on different types of obstructions and other heterogeneous domains, which may guide future numerical and experimental studies. These results may also provide new insights into biological pattern growth and formation, especially in non-idealized domains containing noise or discontinuities.

Published under an exclusive license by AIP Publishing. https://doi.org/10.1063/5.0099753

Turing's mechanism for pattern formation resulting from the interaction of reaction and diffusion is a key paradigm in the theory of morphogenesis. Most model studies of Turing patterns have utilized static, uniform domains, but patterns in living organisms typically develop on growing domains (cells, tissues, animal skins,...), which may contain regions that inhibit or prevent pattern formation. Here, in a chemically realistic reaction-diffusion model, we explore the effects of various shapes of obstacles, such as blocks, walls, and slits, on Turing patterns that arise on growing domains. We identify how such obstructions can affect the mode of growth and how that behavior changes with the growth rate.

I. INTRODUCTION

One of the most fascinating and long-standing open problems in developmental biology is that of embryonic patterning: How can an initially homogeneous embryo develop into a complex heterogeneous organism with many localized substructures? Or, perhaps more importantly, how does the embryo do so reliably? Despite the existence of noise and other inhomogeneities present throughout all stages of development, embryos and stem cells differentiate into

well-maintained structures in an extremely reproducible manner, often referred to as morphogenesis.

Over the past century, biologists have attempted to understand the phenomenon of morphogenesis. Two major theories have arisen:² positional information (sometimes referred to as the French flag model),1-3 where a simple linear gradient of a signaling molecule leads to distinct concentration-dependent gene expression regions; 1,4,5 and Turing's reaction-diffusion mechanism, where patterning can spontaneously arise from the interaction between two morphogens (usually a self-activator and an inhibitor) via a diffusion-driven instability.⁶⁻⁸ Both mechanisms have been implicated in a wide variety of biological systems. For example, positional information has been indicated as an underlying mechanism of molecular patterning in *Drosophila* embryos,²⁻⁵ chick wing bud formation,^{2,9} and the C. elegans germline.¹⁰ Meanwhile, a Turingtype mechanism has been implicated in biological phenomena, such as fish skin patterning,11-14 lung morphogenesis,15 brain folding,16 and leopard spot formation. 17-19 A Turing mechanism has also been suggested in ecological and behavioral phenomena, such as ant nest formation,²⁰⁻²² desertification of arid ecosystems,^{23,24} and even the distribution of criminal activity in cities.25

As more and more systems that undergo morphogenesis are linked to either positional information or the Turing mechanism,

researchers have begun studying how other biological phenomena affect the two models of pattern development. Growth, which is an essential component of any living system, is of particular interest. Growth has been shown to make the patterning resulting from both positional information 4.5,26 and Turing mechanism 27-31 systems more robust to changes in biological or chemical reaction rates. Growth also significantly influences pattern development and morphology. 4,26,27,31-36

However, in many of the studies on the interaction of growth and morphogenetic patterning, growth occurs in an idealized, uniform manner, either apically (growth along one central axis)^{26,32,34} or isotropically (uniform growth in all directions).^{29,35–37} Recently, researchers have begun to investigate heterogeneous growth and growth with spatial discontinuities. In this regard, the study of positional informational systems is more advanced than that of the Turing mechanism. Real biological systems with morphogenesis linked to positional information have shown fascinating and complex behavior with these types of imperfect growth. For example, researchers studying *Drosophila* embryos have shown that spatially discontinuous gradients of the *omb* gene can cause a retraction of cells in the wing imaginal disk, leading to a loss of function.³⁸ In another system, a semi-permeable diffusion barrier can lead to increased pattern robustness in the gonad of *C. elegans*.^{10,39}

Most of the research into Turing patterns (spatial patterns resulting from the Turing mechanism) growing on nonuniform domains involves either a spatially dependent reaction and/or diffusion parameters^{27,40,41} or smoothly curved nonuniform domain boundaries.^{33,42} To the authors' knowledge, only one previous study has been done on Turing pattern growth on a strongly nonuniform domain.⁴³ In this study, Crampin *et al.* showed that nonuniform growth can lead to multiple new pattern morphologies beyond those obtained with uniform domain growth. Primarily, they showed that on a one-dimensional domain, strongly nonuniform growth can disrupt normal peak-splitting behavior.⁴³

In this paper, our objective is twofold: we seek to (a) extend some of the results of Crampin et al.43 to a physically meaningful model on a two-dimensional spatial domain with realistic parameters and (b) examine a variety of novel patterns that are possible with Turing pattern growth on domains with discontinuities. We use the Lengyel-Epstein (LE) model, which was developed to describe the behavior of the chlorine dioxide-iodine-malonic acid (CDIMA) chemical reaction. 44,45 The CDIMA reaction is particularly important in the study of Turing patterns, as it was the first experimental system to conclusively show such patterns—almost 40 years after Turing first proposed their existence.⁴⁶⁻⁴⁸ The LE model has been shown to accurately depict the Turing patterns found in the CDIMA reaction in numerous past studies, including pattern resonance under periodic forcing, 49,50 multifold pattern wavelength increases,5 one-dimensional growth,34 and, most recently, two-dimensional uniform radial growth.35,36

In this study, we investigate the formation of Turing patterns primarily in the presence of three types of obstructions: small blocks that the Turing pattern grows to envelop, uniform walls, and walls with a small slit removed. While this work does not reveal all of the possible behaviors a growing Turing pattern might exhibit in the presence of obstructions, it does provide a systematic methodology that could be used for any obstruction geometry. The results

of this research will bring the study of pattern growth via a Turing mechanism toward the level of understanding we have of growing positional information patterns on nonuniform domains. This research may also provide insights into how discrete spatial obstructions can affect Turing patterns in systems where a Turing-type mechanism has been implicated, such as arid ecosystem desertification or the morphogenesis of the lung.

II. MODEL

We utilize the Lengyel–Epstein two-variable model,⁴⁵ which is given by Eqs. (1) and (2):

$$\frac{\partial u}{\partial \tau} = a - u - \frac{4uv}{1 + u^2} + \nabla^2 u,\tag{1}$$

$$\frac{\partial v}{\partial \tau} = \sigma \left[b \left(u - \frac{uv}{1 + u^2} \right) + d\nabla^2 v \right],\tag{2}$$

where u and v are variables corresponding to the concentrations of the activator (I⁻ in the CDIMA reaction) and inhibitor (ClO $_2^-$ in the CDIMA reaction), respectively. τ is time, and a and b are parameters associated with initial concentrations and rate constants. d is the diffusion ratio of the inhibitor to the activator, and σ is a parameter associated with the immobilization of the activator in the gel, which contributes to the effective difference in diffusion rates. Parameter values used in our simulations are a=12, $\sigma=50$, and d=1. A range of b values from 0.29 to 0.35 was used to generate a variety of pattern morphologies. Higher b favors the formation of spots over stripes. b=0.31 is used, unless otherwise stated, in most of our simulations. All variables and parameters are dimensionless.

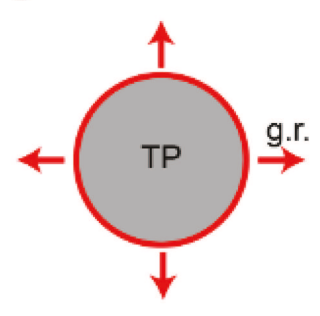
III. METHODS

Equations (1) and (2) were solved numerically using a finite element method (FEM) geometry and a backward differentiation formula (BDF) time-dependent solver implemented in COMSOL Multiphysics version 5.5. The schemes for the simulations are depicted in Fig. 2. The obstruction boundary and the exterior of the patterning region are defined by Neumann zero-flux boundaries. The growth is conducted on a circular domain. In the growth simulations, the radius of the pattern-forming domain increases such that the entire zero-flux boundary moves outward. The initial conditions of model variables are set to v(x,y) = 4 and u(x,y) = 2 +/- rnd(x,y), where rnd(x,y) is a uniformly distributed random number between 0 and 1. When the radius of the domain is increased, the variables u and v start with zero values in the expanding domain. No chemical species are present inside the boundary of the obstructions.

The control simulations (Fig. 1) consist of three sets: First [Fig. 1(a)], we perform simulations with no growth and no obstructions. In these simulations, the domain is set to the final size and allowed to form an unforced Turing pattern for 1000 time units (t.u.) beginning from the aforementioned uniformly distributed random conditions. The second control set [Fig. 1(b)] consists of growing Turing patterns with no obstructions. The initial domain size is very small (radius 0.1 dimensionless space units, s.u.), far less than the pattern wavelength, which is approximately 7 s.u. The radius of the domain is then increased by 0.5 s.u. and simulated for the



(a) No growth and no obstructions.



(b) Growth without obstructions.



(c) Obstructions without growth.

FIG. 1. Schemes for control simulations. Bold black lines designate fixed boundaries; the red line designates a moving boundary. All boundaries are zero-flux. The shaded gray areas indicate regions, where u and v are nonzero and Turing patterns form. In the white areas, no Turing patterns form and no FEM mesh is applied. (a) Turing pattern (TP) formation without growth and without obstructions. The pattern-forming area remains fixed, and Turing patterns are allowed to develop for 1000 t.u. (b) Turing pattern formation on a growing domain without obstructions. The domain starts at a very small initial width or radius (0.1 s.u.) and then grows at varying growth rates (g.r.) to a maximum radius of 100 s.u. (c) Turing pattern formation with obstructions but without growth. The Turing patterns are allowed to form for 1000 t.u., while the domain is at the maximum radius with the obstructions present.

appropriate amount of time with this size to achieve a desired growth rate. These simulations are analogous to previous work on Turing pattern formation in growing systems. 34,35 The last set of control simulations [Fig. 1(c)] is the formation of Turing patterns

with obstructions but without growth. The Turing pattern-forming domain is set to the maximum size (with the obstructions present) and allowed to form a Turing pattern for 1000 t.u. without growth.

For simulations with obstructions and growth (Figs. 3–6), the obstructions are placed to the right of the origin or arrayed around the center in the case of circular obstructions. The time-dependent solver simulates the Turing pattern at a small fixed size for a selected period of time that we call time step. Then, the system radius is increased by 0.5 s.u., after which the simulations continue for another time step. The growth rate of the pattern is the space step, which is always 0.5 s.u., divided by the time step. The growth continues until the radius has reached the final size of 100 s.u. The finite element mesh is reconstructed each time the system grows in size. The shape of the obstructions is "subtracted" from the geometry when the mesh is constructed so that the shape of the domain where patterns form is a circle with the obstruction "cut" from it; see Fig. 2.

We note that this approach differs from the model for growth we have utilized in our previous work,³⁵ where there were two domains, an illuminated domain where the Turing patterns are suppressed, and a dark domain where Turing patterns form. While the two-domain model is closer to the experimental system, the effect of the dark/light domain boundary has an obscuring effect on pattern orientation and growth modes. We have demonstrated previously that the one-domain scheme employed here shows similar pattern trends without obscuring boundary effects.³⁶

IV. RESULTS

A. Obstructions in a system with a fast growth rate

In the radial system with no obstruction and a fast growth rate of 1.0 s.u./t.u. (space units per time units), a Turing pattern forms in the shape of concentric rings parallel to the growing boundary (Fig. 3, leftmost image). This growth mode is called outer ring addition (ORA).³⁵

Our simulations show that the symmetry of the ORA mechanism is broken when the growing system encounters an obstruction. The block-type obstruction simulations produce localized effects on the TP formation (Fig. 3). The obstruction has a "wake" that increases in size, causing pattern disruptions that quickly propagate outward as the system grows. The closer the block obstruction is to the system center, the stronger is the pattern disruption. The outer ring addition stripe pattern breaks down after the obstruction interferes with the pattern growth and is replaced by perpendicular stripes or a mixture of perpendicular stripes and spots behind the obstruction.

With the wall-type obstruction, one might anticipate little or no interaction between the regions on either side of the wall. However, when the wall is located near the system center, the obstruction has a strong effect on the pattern formation. The stripes immediately before of the wall are parallel to the wall obstruction, while on the other side, behind the wall, there is perpendicular pattern growth (bottom "wall" image in Fig. 3). When the wall obstruction is more than about five wavelengths from the pattern center, the ORA growth mode before the wall is practically unaffected by the presence of the wall. The pattern behind the wall is always perpendicular to the direction of growth; i.e., the stripes are directed radially, regardless of the location of the wall.

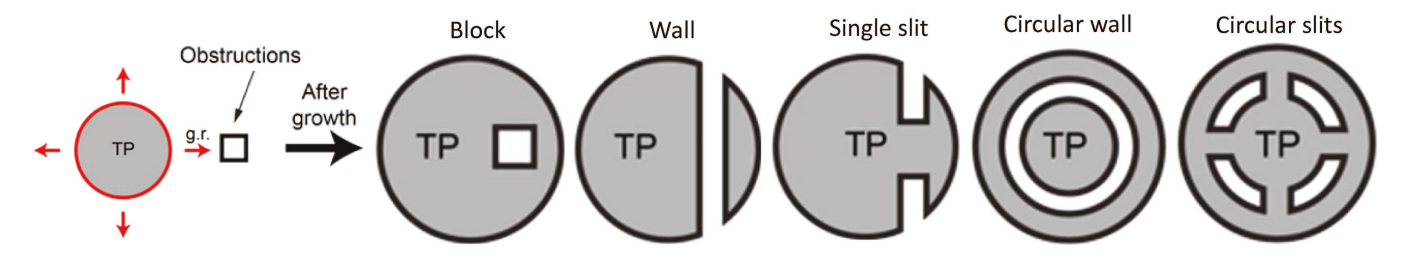


FIG. 2. Schemes for growing Turing patterns with domain obstructions. The leftmost scheme depicts the growth of the Turing patterns before the pattern encounters an obstruction. The red boundary represents a moving non-zero flux boundary. The schemes to the right of the large arrow display the final system geometry with the utilized obstruction. The block obstruction consists of a single 10×10 s.u. square in the vertical center of the domain, offset from the system center by 10, 20, 30, or 60 s.u. The wall-type obstruction is a 10 s.u. thick vertical slice stretching across the entire domain. The single-slit obstruction is identical to the wall obstruction, except an additional 10×10 s.u. square is removed from the vertical center of the obstruction, forming a slit through which Turing patterns can form. The circular wall obstruction consists of a 5 s.u. thick circular wall. The circular slits are the same as the circular walls, but with four 10 s.u. wide gaps formed in the wall at intervals of 90° . Note that the geometries are not shown to scale.

Results for the system with a single small slit in the wall obstruction are similar to those observed with full wall obstructions. The slit enables interaction between the two domains, but the wall obstruction dominates, and the pattern behind and in front of the slit obstruction is nearly unaffected by the slit opening in the wall.

The circular wall obstruction produces interesting patterns. When the radius of the wall is smaller than two pattern wavelengths, the ORA growth mode is preserved inside and outside the obstruction. At wall radii above two wavelengths, the ORA mode persists only inside the obstruction, while on the outside, perpendicular stripes form. Similar results are obtained for the circular wall obstruction with four slits (last column in Fig. 3).

B. Obstructions in a system with an intermediate growth rate

At the intermediate growth rate of 0.5 s.u./t.u., the growth mode begins to switch from ORA to perpendicular pattern growth (PPG).³⁵ After an initial period of ORA growth, stripes start to form

at the growth boundary and expand outward, orthogonal to the growing circle. This transition can be seen in the animations in the supplementary material.

Once the concentric ring TP has given way to these orthogonal stripes, the small block obstacle does not appear to have a significant impact on the resulting pattern, as shown in Fig. 4. The stripes grow around the obstacle and continue the PPG mode. However, if the obstruction is within the ORA initial growth regime, such as 10 s.u. from the center (Fig. 4, bottom left), the ring symmetry is broken and the growth mode immediately switches to PPG.

The wall and single-slit obstructions also do not significantly change the PPG mode. Once the patterns begin to form perpendicular to the growing boundary, the wall obstacle simply blocks the patterns from growing further, and PPG continues on the other side of the obstruction, as with the faster growth rate.

The radially oriented obstructions similarly do not strongly change the pattern growth. For the ring obstructions with medium radii, ring TPs form in their center and perpendicular stripes form

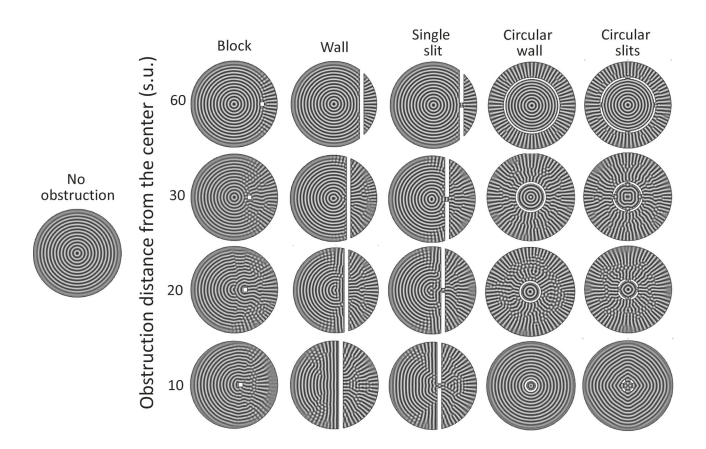


FIG. 3. Turing patterns with a fast growth rate of 1.0 s.u./t.u. and obstructions placed at different distances from the system center. Images show a pattern when the system reaches its maximum radius of 100 s.u.

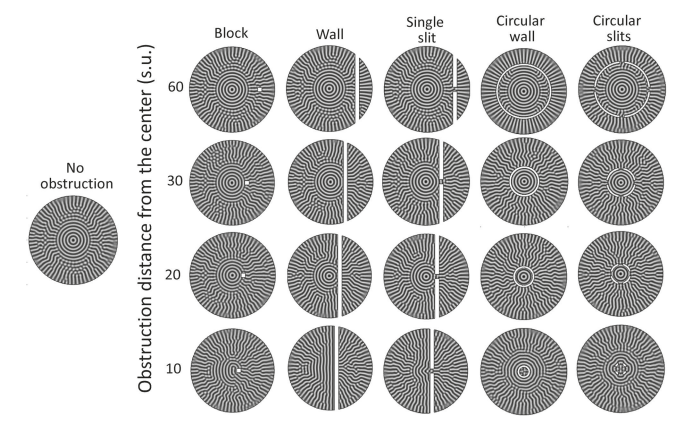


FIG. 4. Turing patterns at an intermediate growth rate of 0.5 s.u./t.u. and obstructions placed at different distances from the system center. Images show a pattern when the system reaches its maximum radius of 100 s.u.

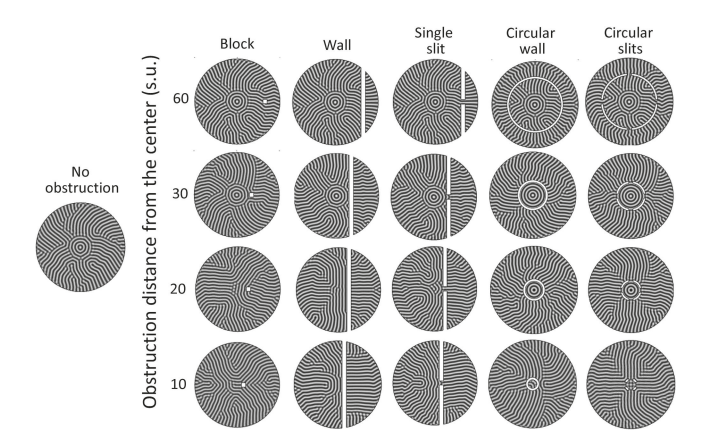


FIG. 5. Turing patterns at a slow growth rate of 0.1 s.u./t.u. and obstructions placed at different distances from the system center. Images show pattern when the system reaches its maximum radius of 100 s.u.

beyond them. When the ring is too small to allow for more than one pattern wavelength to form, rings form around the obstruction, as shown in the bottom right of Fig. 4.

C. Obstructions in a system with a slow growth rate

For extremely slow growth rates, TP grow first by expanding as the domain grows, with new wavelengths emerging in the center of the domain. We have termed this phenomenon inner ring growth (IRG). Although the resulting concentric rings appear similar to those from the ORA growth mode, they emerge in a very different

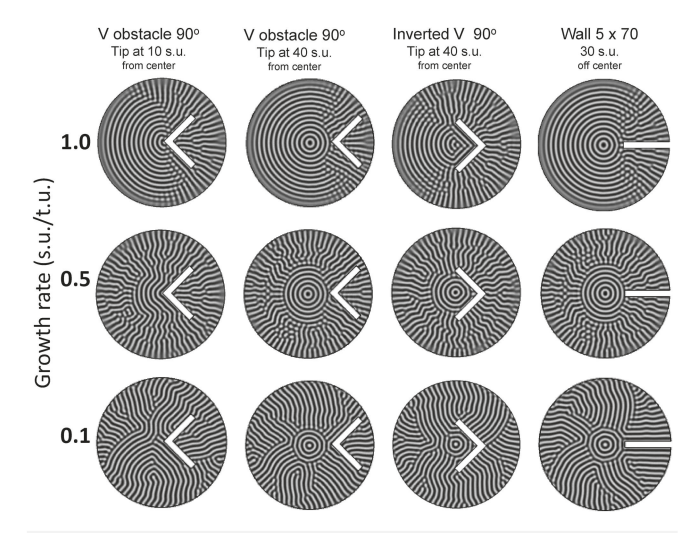


FIG. 6. Turing patterns at high, intermediate, and low growth rates with V-shaped and perpendicular line-shaped obstructions. The thickness of obstructions is 10 s.u. Each arm of the V-shaped obstruction is 50 s.u. long, and the line-shaped obstruction is 70 s.u. long. Images show a pattern when the system reaches its maximum radius, 100 s.u.

manner. This can be seen in the animation in the supplementary material. As shown in Fig. 5, once the domain grows past a certain radius, the concentric rings break into perpendicular stripes and grow via the PPG mode.

Generally, obstructions have a greater impact on the patterns that form via IRG. When the blocks are close to the center, once the domain reaches the center, the TP ring symmetry is immediately split. However, as the growth is occurring more slowly than the relevant chemistry, the pattern has sufficient time to completely re-form, removing any trace of the original ring symmetry. This is shown for obstructions 10 or 20 s.u. from the origin of the growing domain in Fig. 5.

The wall, single-slit, circular-wall, and circular-slit obstructions behave much as they do with the intermediate growth rates. In general, if the obstruction (regardless of the orientation) is sufficiently close to impact the patterns formed through IRG, any vestige of the ring symmetry will be eliminated as the pattern is given sufficient time to reorient during the slow growth. When the growing domain becomes large enough to naturally break down into perpendicular patterns, the obstructions cause the patterns to behave as for faster growth rates (Figs. 3 and 4).

D. Other obstructions

Obstructions with different geometries were also studied to determine the impact of the obstruction's geometry and its location relative to the origin of the growing domain. As shown in the first two columns of Fig. 6, regardless of the domain growth rate, the closer the obstacle is to the origin of the growing domain, the greater its impact on the TP morphology. When the tip of the V obstacle is 10 s.u. from the center of the domain, no concentric rings can form. When the tip is 40 s.u. from the center of the domain, for fast and intermediate growth rates, concentric ring TPs form until the domain grows into the obstacle, where the rings abruptly break apart. For the slow growth rate, the concentric rings from the IRG growth mode naturally rupture prior to interacting with the obstruction. For the inverted V obstacle (3rd column of Fig. 6), the concentric rings fracture as soon as the system intersects with the obstruction, which in Fig. 6, column 3, is about 20 s.u. from the origin.

The geometry of the obstruction has a smaller effect on the TP morphology. However, for slow growth rates (such as 0.1 s.u./t.u. in Fig. 6), this effect is non-negligible. For the perpendicular line obstruction, the TP forms near the obstruction as stripes parallel to the wall. This also occurs somewhat for the V obstacles. When the TP emerges on the other side of the obstruction, such as for the inverted V, patterns form orthogonal to the obstruction boundary. For faster growth rates, the patterns do not adjust as markedly to the obstruction boundary.

V. DISCUSSION AND CONCLUSION

Our results indicate that the formation of Turing patterns is strongly influenced by the presence of obstructions. Growth is necessary for the effect of the obstructions. Obstructions placed on domains where Turing patterns are formed without growth show little interaction between the pattern and the obstruction; see Fig. 7.

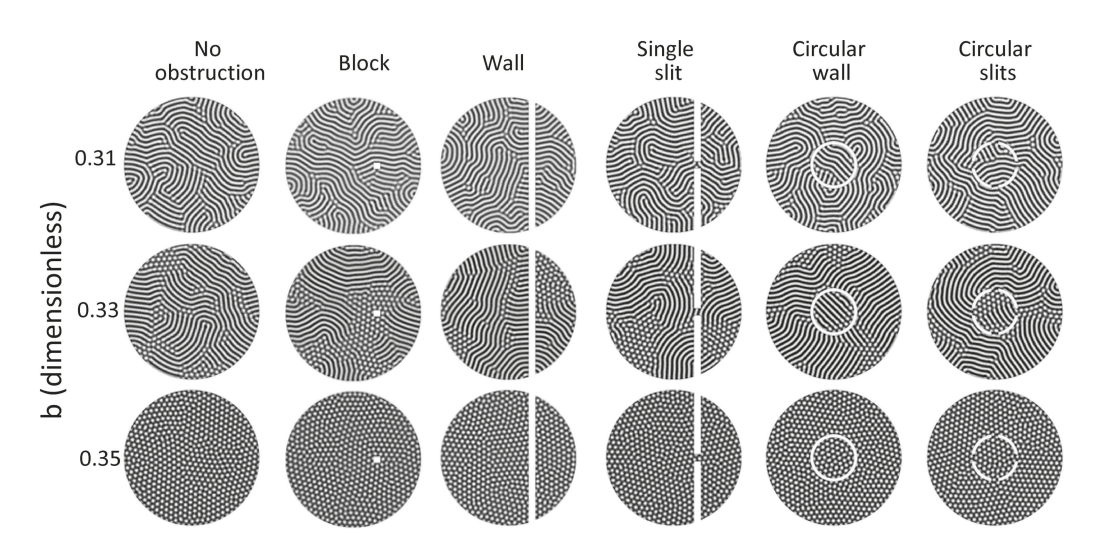


FIG. 7. Results for control simulations with obstructions, but no growth. Obstructions are placed within the domain, and Turing patterns are allowed to form around them.

Our simulations of radial growth highlight that the effect is strongly geometry-dependent, with both the location of the obstacle relative to the origin of the growing domain and the shape of the obstacle playing major roles. For TP arising via the ORA and IRG modes, once the concentric ring patterns encounter an obstruction, the rings' symmetry breaks immediately. For intermediate and slower growth, the patterning over the entire domain then switches to the PPG mode. Partial ring symmetry (for example, TP shown in Fig. 3) is only maintained for fast growth rates. These results indicate that discrete obstructions in the domain favor the PPG mode over a much wider region in parameter space (the parameter space on uniform domains is given in Ref. 35). Future research might explore whether other types of domain nonuniformities (such as morphogen gradients 52) would similarly impact Turing pattern formation on growing domains to favor the PPG mode.

When the growing domain beyond the obstruction has a connection to the initial domain through a slit, there is an increased propensity for the Turing pattern observed to match that before the obstruction near the slit or for an entirely different pattern to be observed close to the obstruction due to the pattern interactions. For the narrow slits shown in Figs. 3–5, the patterns closely resemble those found with a wall obstacle at the same distance from the center, particularly when the slit obstacle is placed far from the center (30 or 60 s.u.). When the obstacle is located 20 s.u. or less from the center, a small local disturbance in the pattern may be seen immediately in front of the slit. We explore the effect of widening the slit at slow growth rates and show in Fig. 4 of the supplementary material that slit widths above about five pattern wavelengths produce more significant changes in the direction of the post-slit stripes.

We also tested how the space/time steps used to generate the moving boundaries affect the pattern formation in the growing systems with obstacles. We observed that for a space step of 0.5 s.u. or smaller, the results are independent of the selected step for the growth rates investigated. However, when the time step is fixed at 10 t.u. and the radius of the domain is increased by the appropriate space step to yield a selected growth rate, at some growth rates, the pattern depends on the space step. At higher growth rates, the space step becomes comparable to the pattern wavelength, and the pattern tends to preserve its symmetry even after an encounter with an obstruction. However, when the space step is kept small (0.5 s.u. and smaller) by reducing the time step, the presence of obstructions breaks the pattern symmetry, as shown in Fig. 8.

Importantly, the effects of the obstructions are for the most part limited to the portion of the pattern that forms after the moving boundary contacts the obstruction. As expected, Turing patterns already formed behind the obstruction do not shift noticeably to accommodate the obstruction since Turing patterns are temporally stable. Conversely, patterns that form close to or behind the obstruction are strongly influenced by its presence. This observation is consistent with the results of Crampin *et al.*, which show that in the case of a one-dimensional domain, defects in the peak-splitting behavior of a growing Turing system only occur near the edge of the growing boundary.⁴³

The results presented in this work demonstrate that the formation of biologically relevant Turing patterns is strongly influenced by the combination of growth and domain shape. In the absence of growth (Fig. 7), we observe randomly oriented patterns. The presence of obstructions in a growing domain (Figs. 3–6) has a significant effect on pattern orientation. The obstructions have the highest propensity to induce growth mode changes at intermediate growth rates. Since intermediate growth rates are where changes in patterning modalities are observed without obstructions, this indicates that domain obstructions cause shifts in observed pattern morphologies.

Since growth in biological systems rarely occurs on fully homogeneous domains, this work may provide new insights into

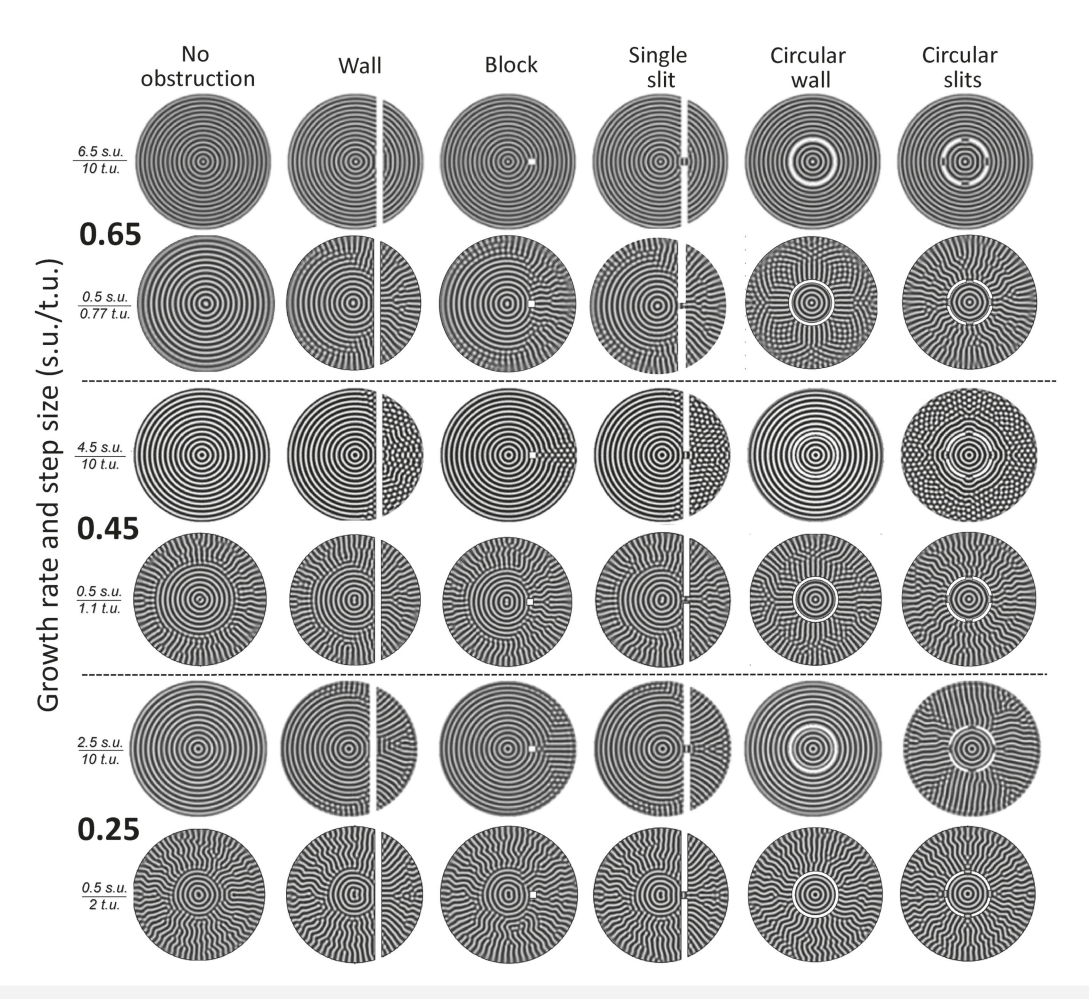


FIG. 8. Effect of the step size on growing Turing patterns.

morphogenesis. Future work on this topic may investigate the behavior of additional types of obstructions, obstacles, or domains with preexisting morphogen gradients, as well as construct systems to test the effect of obstructions on Turing pattern growth experimentally. One could attempt to do this using the chlorine dioxide-iodine-malonic acid (CDIMA) reaction in an unstirred system, as in our previous study on a homogeneous domain.³⁵ Using light to control the growth will allow for control over the growing domain. However, significant care would have to be taken to ensure reproducibility with regard to obstacle placement and distance from the origin of the growing domain. Other promising directions for further research include exploring the effects of multiple obstacles and probing the effects of obstacles on Turing patterns in three dimensions. Earlier research by Bansagi et al. unveiled a wide range of experimentally verifiable three-dimensional Turing patterns, yet little work has been done to analyze their robustness or how they are affected by obstructions in the patterning region.⁵³ Simulations of this and other patterning systems may lead to new insights into the behaviors of Turing patterning systems on nonuniform domains.

SUPPLEMENTARY MATERIAL

See the supplementary material that contains parameter sweeps of wider ranges of b values utilizing the obstructions described in this work, as well as additional obstacle types. It also contains a fine sweep of the geometry of the single-slit type obstacle. Additionally, selected animations of Turing pattern growth and the finite element mesh are provided.

ACKNOWLEDGMENTS

The authors thank Vaclav Klika for enlightening discussions of growth and pattern formation. N.H.S. is grateful to Daniel Farb for his meaningful insights. We acknowledge financial support from the National Science Foundation (No. NSF CHE-1856484) and the M.R. Bauer Foundation. We extend our best wishes to Dick Field on the occasion of his 80th birthday.

AUTHOR DECLARATIONS

Conflict of Interest

The authors have no conflicts to disclose.

Author Contributions

Milos Dolnik: Investigation (supporting); Supervision (supporting); Writing - review and editing (equal). Christopher Konow: Investigation (supporting); Software (supporting); Writing - original draft (supporting); Writing - review and editing (supporting). Noah H. Somberg: Investigation (supporting); Software (lead); Writing original draft (supporting). Irving R. Epstein: Conceptualization (equal); Funding acquisition (lead); Investigation (equal); Project administration (lead); Resources (lead); Supervision (lead); Writing - review and editing (equal).

DATA AVAILABILITY

The data that support the findings of this study are available from the corresponding author upon reasonable request.

REFERENCES

- ¹L. Wolpert, "One hundred years of positional information," Trends Genet. 12,
- ²J. B. Green and J. Sharpe, "Positional information and reaction-diffusion: Two big ideas in developmental biology combine," Development 142, 1203-1211
- ³L. Wolpert, "Positional information and the spatial pattern of cellular differentiation," J. Theor. Biol. 25, 1-47 (1969).
- ⁴K. D. Irvine and C. Rauskolb, "Boundaries in development: Formation and function," Annu. Rev. Cell Dev. Biol. 17, 189-214 (2001).
- ⁵H. L. Ashe and J. Briscoe, "The interpretation of morphogen gradients," Development 133, 385-394 (2006).
- ⁶A. M. Turing, "The chemical basis of morphogenesis," Philos. Trans. R. Soc. B: Biol. Sci. 237, 37-72 (1952).
- ⁷A. Gierer and H. Meinhardt, "A theory of biological pattern formation," Kybernetik 12, 30-39 (1972).
- ⁸H. Meinhardt and A. Gierer, "Pattern formation by local self-activation and lateral inhibition," BioEssays 22, 753-760 (2000).
- ⁹J. W. Saunders and M. T. Gasseling, "Ectodermal-mesenchymal interactions on the origins of wing symmetry," in Epithelial-Mesenchymal Interactions (William & Wilkins, Baltimore, MD, 1968), pp. 78–97.
- ¹⁰A. Cinquin, L. Zheng, P. H. Taylor, A. Paz, L. Zhang, M. Chiang, J. J. Snow, Q. Nie, and O. Cinquin, "Semi-permeable diffusion barriers enhance patterning
- robustness in the *C. elegans* germline," Dev. Cell **35**, 405–417 (2015).

 11 S. Kondo and R. Asai, "A reaction–diffusion wave on the skin of the marine angelfish Pomacanthus," Nature 376, 765-768 (1995).
- 12 S. Kondo and T. Miura, "Reaction-diffusion model as a framework for understanding biological pattern formation," Science 329, 1616-1620 (2010).
- ¹³D. Bullara and Y. De Decker, "Pigment cell movement is not required for generation of Turing patterns in zebrafish skin," Nat. Commun. 6, 6971 (2015). ¹⁴C. Konow, Z. Li, S. Shepherd, D. Bullara, and I. R. Epstein, "Influence of sur-
- vival, promotion, and growth on pattern formation in zebrafish skin," Sci. Rep. 11, 9864 (2021).
- 15 Y. Guo, M. Sun, A. Garfinkel, and X. Zhao, "Mechanisms of side branching and tip splitting in a model of branching morphogenesis," PLoS One 9, e102718
- ¹⁶J. Lefèvre and J. F. Mangin, "A reaction-diffusion model of human brain development," PLoS Comput. Biol. 6, e1000749 (2010).
- ¹⁷R. T. Liu, S. S. Liaw, and P. K. Maini, "Two-stage Turing model for generating pigment patterns on the leopard and the jaguar," Phys. Rev. E 74, 011914

- ¹⁸J. D. Murray, "How the leopard gets its spots," Sci. Am. 258, 80-87 (1988).
- ¹⁹A. J. Koch and H. Meinhardt, "Biological pattern formation: From basic mechanisms to complex structures," Rev. Mod. Phys. **66**, 1481–1507 (1994).

 ²⁰G. Theraulaz, E. Bonabeau, and J.-L. Deneubourg, "The origin of nest complex-
- ity in social insects," Complexity 3, 15-25 (1998).
- ²¹G. Theraulaz, E. Bonabeau, S. C. Nicolis, R. V. Solé, V. Fourcassié, S. Blanco, R. Fournier, J. L. Joly, P. Fernández, A. Grimal, P. Dalle, and J. L. Deneubourg, "Spatial patterns in ant colonies," Proc. Natl. Acad. Sci. U.S.A. 99, 9645-9649
- ²²G. Theraulaz, J. Gautrais, S. Camazine, and J. L. Deneubourg, "The formation of spatial patterns in social insects: From simple behaviours to complex structures," Philos. Trans. Royal Soc. A 361, 1263-1282 (2003).
- ²³E. Meron, E. Gilad, J. von Hardenberg, M. Shachak, and Y. Zarmi, "Vegetation patterns along a rainfall gradient," Chaos, Solitons Fractals 19, 367-376
- ²⁴R. Hille Ris Lambers, M. Rietkerk, F. V. D. Bosch, H. H. T. Prins, and H. D. Kroon, "Vegetation pattern formation in semi-arid grazing systems," Ecology 82, 50-61 (2001).
- ²⁵ M. B. Short, P. J. Brantingham, A. L. Bertozzi, and G. E. Titad, "Dissipation and displacement of hotspots in reaction-diffusion models of crime," Proc. Natl. Acad. Sci. U.S.A. 107, 3961-3965 (2010).
- ²⁶P. Rinne and C. van der Schoot, "Symplasmic fields in the tunica of the shoot apical meristem coordinate morphogenetic events," Development 125, 1477-1485
- (1998).

 27 R. Plaza, F. Sanchez-Garduno, P. Padilla, R. A. Barrio, and P. K. Maini, "The formation" J. Dvn. Differ. Equ. 16, effect of growth and curvature on pattern formation," J. Dyn. Differ. Equ. 16, 1093-1121 (2004).
- ²⁸ A. D. Economou, A. Ohazama, T. Porntaveetus, P. T. Sharpe, S. Kondo, M. A. Basson, A. Gritli-Linde, M. T. Cobourne, and J. B. Green, "Periodic stripe formation by a Turing mechanism operating at growth zones in the mammalian palate," Nat. Genet. 44, 348-351 (2012).
- ²⁹ A. Madzvamuse, E. A. Gaffney, and P. K. Maini, "Stability analysis of nonautonomous reaction-diffusion systems: The effects of growing domains," J. Math. Biol. 61, 133-164 (2010).
- ³⁰V. Klika and E. A. Gaffney, "History dependence and the continuum approximation breakdown: The impact of domain growth on Turing's instability," Proc. R. Soc. A: Math. Phys. Eng. Sci. 473, 20160744 (2017).
- ³¹ A. A. Neville, P. C. Matthews, and H. M. Byrne, "Interactions between pattern formation and domain growth," Bull. Math. Biol. 68, 1975-2003 (2006).
- 32D. M. Holloway and L. G. Harrison, "Pattern selection in plants: Coupling chemical dynamics to surface growth in three dimensions," Ann. Bot. 101, 361-374 (2007).
- 33 R. A. Barrio, C. Varea, J. L. Aragón, and P. K. Maini, "A two-dimensional numerical study of spatial pattern formation in interacting Turing systems," Bull. Math. Biol. 61, 483-505 (1999).
- ³⁴D. G. Míguez, M. Dolnik, A. P. Muñuzuri, and L. Kramer, "Effect of axial growth on Turing pattern formation," Phys. Rev. Lett. 96, 048304 (2006).
- 35 C. Konow, N. H. Somberg, J. Chavez, I. R. Epstein, and M. Dolnik, "Turing patterns on radially growing domains: Experiments and simulations," Phys. Ch Chem. Phys. 21, 6718-6724 (2019).
- ³⁶N. H. Somberg, C. Konow, I. R. Epstein, and M. Dolnik, "Growth mode selection of radially growing Turing patterns," in Proceedings of the COMSOL Users Conference Boston (Brandeis University, 2019); available at https://www.comsol. om/paper/growth-mode-selection-of-radially-growing-turing-patterns-81501.
- ³⁷A. Madzvamuse and P. K. Maini, "Velocity-induced numerical solutions of reaction-diffusion systems on continuously growing domains," J. Comput. Phys. **225**, 100-119 (2007).
- ³⁸J. Shen, C. Dahmann, and G. O. Pflugfelder, "Spatial discontinuity of optomotor-blind expression in the Drosophila wing imaginal disc disrupts epithelial architecture and promotes cell sorting," BMC Dev. Biol. 10, 23 (2010).
- ³⁹M. A. Miller, "Patterning with diffusion barriers," Dev. Cell 35, 395–396 (2015).
- ⁴⁰ K. Page, P. K. Maini, and N. A. Monk, "Pattern formation in spatially heterogeneous Turing reaction-diffusion models," Physica D 181, 80-101 (2003).
- ⁴¹ M. Bengfort, H. Malchow, and F. M. Hilker, "The Fokker-Planck law of diffusion and pattern formation in heterogeneous environments," J. Math. Biol. 73, 683-704 (2016).

- ⁴²M. J. Simpson, K. A. Landman, and D. F. Newgreen, "Chemotactic and diffusive migration on a nonuniformly growing domain: Numerical algorithm development and applications," J. Comput. Appl. Math. 192, 282–300 (2006).
 ⁴³E. J. Crampin, W. W. Hackborn, and P. K. Maini, "Pattern formation in
- ⁴³E. J. Crampin, W. W. Hackborn, and P. K. Maini, "Pattern formation in reaction-diffusion models with nonuniform domain growth," Bull. Math. Biol. **64**, 747–769 (2002).
- 747–769 (2002).

 44I. Lengyel, G. Rábai, and I. R. Epstein, "Experimental and modelling study of oscillations in the chlorine dioxide-iodine-malonic acid reaction," J. Am. Chem. Soc. 112, 9104–9110 (1990).
- ⁴⁵I. Lengyel and I. R. Epstein, "Modeling of Turing structures in the chlorite-iodide-malonic acid-starch reaction system," Science **251**, 650–652 (1991).
- ⁴⁶V. Castets, E. Dulos, J. Boissonade, and P. De Kepper, "Experimental evidence of a sustained standing Turing-type nonequilibrium chemical pattern," Phys. Rev. Lett. **64**, 2953–2956 (1990).
- ⁴⁷I. Lengyel and I. R. Epstein, "A chemical approach to designing Turing patterns in reaction-diffusion systems," Proc. Natl. Acad. Sci. U.S.A. 89, 3977–3979 (1992).

- ⁴⁸P. Ball, "Forging patterns and making waves from biology to geology: A commentary on Turing (1952) 'The chemical basis of morphogenesis'," Philos. Trans. R. Soc. B: Biol. Sci. **370**, 20140218 (2015).
- ⁴⁹M. Dolnik, T. Bánsági, Jr., S. Ansari, I. Valent, and I. R. Epstein, "Locking of Turing patterns in the chlorine dioxide-iodine-malonic acid reaction with one-dimensional spatial periodic forcing," Phys. Chem. Chem. Phys. 13, 12578 (2011).
 ⁵⁰D. Feldman, R. Nagao, T. Bánsági, Jr., I. R. Epstein, and M. Dolnik, "Turing
- patterns in the chlorine dioxide-iodine-malonic acid reaction with square spatial periodic forcing," Phys. Chem. Chem. Phys. **14**, 6577 (2012).
- periodic forcing," Phys. Chem. Chem. Phys. 14, 6577 (2012).

 51 D. K. Gaskins, E. E. Pruc, I. R. Epstein, and M. Dolnik, "Multifold increases in Turing pattern wavelength in the chlorine dioxide-iodine-malonic acid reaction-diffusion system," Phys. Rev. Lett. 117, 056001 (2016).
- diffusion system," Phys. Rev. Lett. 117, 056001 (2016).

 52T. Hiscock and S. Megason, "Orientation of Turing-like patterns by morphogen gradients and tissue anisotropies," Cell Syst. 1, 408–416 (2015).
- morphogen gradients and tissue anisotropies," Cell Syst. 1, 408–416 (2015). 53T. Bansagi, Jr., V. K. Vanag, and I. R. Epstein, "Tomography of reaction-diffusion microemulsions reveals three-dimensional Turing patterns," Science 331, 1309–1312 (2011).